Electrochemical behaviour of additively manufactured titanium for biomedical applications

Electrochemical behaviour of additively manufactured titanium for biomedical applications

Alessio Gullino, Sabrina Grassini, Emma Angelini, Elisa Padovano, Claudio Badini, Leonardo Iannucci
Dipartimento di Scienza Applicata e Tecnologia, Politecnico di Torino Torino, ITALY

Marco Parvis
Dipartimento di Elettronica e Telecomunicazioni Politecnico di Torino Torino, ITALY

DOI: 10.1109/MeMeA49120.2020.9137205

Electrochemical behaviour of additively manufactured titanium for biomedical applications

Alessio Gullino
Sabrina Grassini
Emma Angelini
Elisa Padovano
Claudio Badini
Leonardo Iannucci
Dipartimento di di Scienza Applicata e Tecnologia
Politecnico di Torino
Torino, ITALY
Email: leonardo.iannucci@polito.it

Marco Parvis
Dipartimento di Elettronica e Telecomunicazioni
Politecnico di Torino
Torino, ITALY
Email: marco.parvis@polito.it

***Abstract*—Commercially pure titanium is an important material for several biomedical applications, thanks to its capability to promote osseointegration and its mechanical properties. In recent years, new processing routes like additive manufacturing have opened new frontiers in the exploitation of this material in the biomedical field, giving the possibility to realize new shapes and decrease the overall weight of the prostheses. At the same time, due to these new forming technologies, new issues are faced, like the presence of a fine microstructure and the relation between porosity in the final component and the process parameters. This paper employs electrochemical measurements to assess the porosity effect on the corrosion behaviour of additively manufactured titanium in simulated body fluids. Specifically, the possibility of assessing different porosity levels related to processing parameters change is discussed.**

***Index Terms*—Titanium, additive manufacturing, electrochemical measurement, biomaterials**

I. Introduction

Titanium and its alloys play a key role in the field of materials for biomedical applications. Actually, thanks to its biocompatibility, good corrosion resistance and mechanical properties, titanium has been used since decades in many implants [1]. Commercially pure titanium has found application in dental implants (endosseous implants), while titanium alloys are widely used in orthopedics, where better mechanical properties are required. Actually, the good osseointegration and the elastic modulus similar to that of bone make this material the optimal choice for operations like hip or knee replacement [2]–[5]. The good corrosion resistance is related to the presence of a thin ($1.5\ \mathrm{nm} - 10\ \mathrm{nm}$) but continuous oxide layer that covers the metal after exposure to an aerated environment. This passive layer, mainly composed of titanium oxide (TiO_2), is able to protect the material also in harsh environments, such as body fluids [6]. Corrosion rate can increase, leading to dissolution of metallic ions, only if this passivity is lost due to the effect of aggressive species like fluoride ions or hydrogen peroxide [7].

The properties of this material for the biomedical field have also attracted the attention of many researchers involved in the study of additive manufacturing technologies [8]. Actually 3D printing can give the possibility of producing near-net-shape components even when complex geometries are required. Moreover, even if a higher cost must be taken into account, the possibility to obtain custom-made components or the opportunity of lowering the prosthesis total weight is still interesting [9]. For these reasons, many studies have been carried out in the Materials Science field in order to investigate the effects on microstructure of this new processing technology. Specifically, grain size has been found to be affected by the thermal gradients faced by the material during the process and an increase of porosity in the final component has also been reported [10], [11].

This non-homogeneous microstructure can also have an influence on corrosion resistance of the material, with possible detrimental consequences for the biomedical applications of the material. So it is of great importance to find measurement techniques able to assess the electrochemical behavior of the alloy in order to predict its service performance when employed in in-vivo applications. Different studies have investigated the corrosion resistance of alloys produced by 3D printing, comparing it to the performance of the same material obtained by means of traditional techniques such as casting or forging [12]. As far as titanium is concerned, most of the interest has been focused on its alloys, in particular the Ti-6Al-4V, which is widely used in many biomedical applications [15]. To the best of authors' knowledge, the electrochemical behavior of additively manufactured commercially pure titanium has not been investigated yet, despite its important applications for dental implants.

The aim of this work is to characterize the corrosion resistance of commercially pure titanium obtained by 3D printing. Specifically, the correlation between material porosity and results from electrochemical measurements is discussed.

Thus, different process parameters have been tested in order to investigate the most suitable ones to obtain a dense final product. Material porosity was evaluated using an imaging algorithm and then its effect on the electrochemical behavior was assessed using potentiodynamic polarization measurements.

II. Samples production and porosity assessment

Samples under study were produced using the Selective Laser Melting technology, by means of the Concept Laser Mlab Cusing (R) system. Four different processing conditions were chosen, following previous results that can be found in literature [14]. In order to investigate the effect of a single process variable, only the laser scan speed was changed from one sample to the other, keeping all other parameters constant. In this way it is possible to optimize the manufacturing process with a trial-and-error methodology; samples porosity was the parameter used to assess the quality of the final product. The four sets of build parameters are reported in Table I.

Samples were realized in the shape of parallelograms, having dimensions of $10\ \mathrm{mm} \times 10\ \mathrm{mm} \times 12\ \mathrm{mm}$. The printing process quality was evaluated assessing the porosity in the final product, using an imaging analysis. At least 30 micrographs were acquired for each sample using an optical microscope (Leica Mef4). A magnification of $100\times$ was used, so as to have an analyzed area of about $978\ \mu\mathrm{m} \times 734\ \mu\mathrm{m}$. Before observation at optical microscope, specimens were polished on abrasive papers till 4000 grid, rinsed in deionized water, sonicated in ethanol and finally dried.

Acquired micrographs were analyzed in a three-step process. First, porosity was identified using a Machine Learning algorithm, namely the Trainalble Weka Segmentation plugin in Fiji [16], [17]. This is an open source software that allows the user to perform a segmentation of the images after that the algorithm has been trained with a sample image. The user manually select the pixels representing porosities in the micrograph, discriminating them from the rest of the microstructure. In this way, a classifier is created and it can be used to identify the feature of interest, in this case the porosities, also in the other micrographs. After that, images are binarized in order to transform them from gray-scale to binary, i.e. composed only of black or white pixels [18] (see Fig. 1). Finally, the surface percentage occupied by pores and their dimensional distribution can be computed.

Results from the image processing are reported in Table II. As it is possible to see, the laser scan speed has an important influence on the porosity of the final product. Using a higher scan speed (sample A), a high density is obtained, reaching the best results with a scan speed of $900\ \mathrm{mm/s}$. On the contrary, a lower laser scan speed leads to a more porous microstructure, probably due to the higher temperature reached during the process. Using intermediate speed values, a high density is obtained for sample C, while sample B has a surface percentage occupied by pores similar to D.

Interesting information can then be obtained from the analysis of the pores dimensional distribution (Fig. 2).

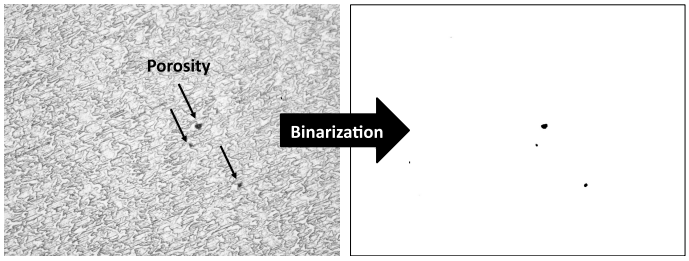

Fig. 1. Example of the result from the image processing for porosity computation: on the left the original micrograph, on the right the binarized image, where pores are identified as black pixels.

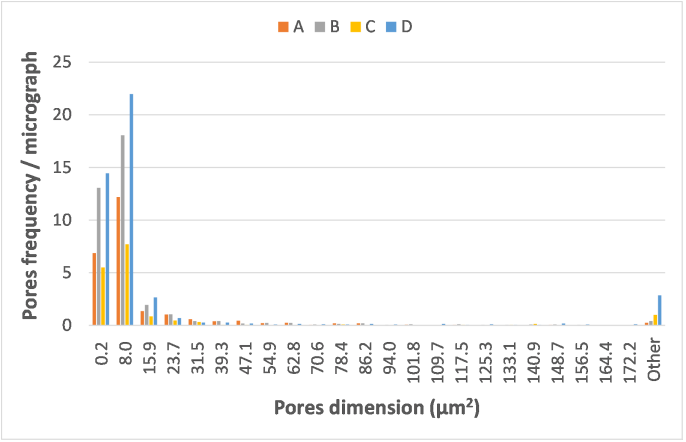

Fig. 2. Pores dimensional distribution.

Actually, it has a trend that is similar for all samples, with a first maximum for pores dimension ranging from $0.2\ \mu\mathrm{m}^2$ to $8.0\ \mu\mathrm{m}^2$, and then a second peak in the class grouping all the pores with an area above $172.2\ \mu\mathrm{m}^2$, which is the last class in the histogram. The first maximum represents pores that are almost regularly distributed in the metal microstructure, like those represented in Fig. 1. On the contrary, the second peak, that is particularly sharp for the D sample, suggests the presence of large pores, which are the most detrimental also as far as mechanical properties are concerned. As their number is notably high for the sample having the lowest laser scan speed, they could be presumably associated to the formation of unstable molten pool during the laser scans [19]. Despite the different surface percentage occupied by pores, the pores average area is similar for samples A, B and C, indicating a similar microstructure. Sample D is characterized by a higher pores average area, as already discussed.

III. Electrochemical measurements

Potentiodynamic polarization measurements have been employed to assess the corrosion behaviours of the different samples and to correlate the obtained results to the computed porosity levels (see Section II). Measurements were carried out using a three-electrode electrochemical cell composed of a counter electrode (a Platinum wire), a reference electrode (Ag/AgCl reference electrode) and a working

TABLE I
PROCESS VARIABLES EMPLOYED TO REALIZE THE SAMPLES UNDER STUDY

Sample	Power [W]	Scan speed [mm/s]	Trace spacing [mm]	Layer thickness [mm]
A	95.0	900	0.098	0.025
B	95.0	600	0.098	0.025
C	95.0	400	0.098	0.025
D	95.0	200	0.098	0.025

TABLE II
POROSITY LEVELS COMPUTED FOR DIFFERENT SAMPLES

	A	B	C	D
Surface percentage occupied by pores	$0.046\% \pm 0.014\%$	$0.160\% \pm 0.133\%$	$0.061\% \pm 0.020\%$	$0.269\% \pm 0.072\%$
Pore average area [μm^2]	18.9 ± 3.4	13.7 ± 1.3	19.2 ± 1.8	33.2 ± 25.3
Average pore number / micrograph	18.3 ± 8.6	80.9 ± 61.7	23.2 ± 9.9	73.7 ± 40.6

electrode (the sample), a common setup for electrochemical measurements [20]. Before the test, samples were prepared as described in Section II. Then, samples were embedded in a polymeric resin in order to have an exposed electrode surface of $10\ \mathrm{mm} \times 10\ \mathrm{mm}$. The present investigation has been carried out recording the polarization curves on the sample plane that is perpendicular to the building direction. The cell was filled with $250\ \mathrm{ml}$ of Hanks' balanced salt solution ($CaCl_2 \cdot 2H_2O$ $0.185\ g/L$, $MgSO_4$ $0.097647\ g/L$, KCl $0.4\ g/L$, KH_2PO_4 $0.06\ g/L$, $NaCl$ $8.0\ g/L$, Na_2HPO_4 $0.04788\ g/L$, D-Glucose$1.0\ g/L$, Phenol Red·Na $0.011\ g/L$, purchased from Sigma-Aldrich®); such electrolyte was chosen in order to simulate a biological environment since its formulation is close to the body fluids one. Potentiodynamic polarization curves were acquired by means of an Ivium-n-Stat potentiostat, in the over-potential range from $-0.7\ \mathrm{V}$ to $+5.0\ \mathrm{V}$ versus the Open Circuit Potential (OCP) with a scan rate of $1\ \mathrm{mV/s}$. The measurement was performed after monitoring for 1 hour the Open Circuit Potential (OCP), in order to have a stable potential of the metal in the solution. All electrochemical measurements were repeated three times on each sample, polishing the metal surface after each test so as to remove any alteration.

The correlation between the exchange current, involved in the potentiodynamic polarization, and the applied over-potential is described by Butler-Volmer equation, as follow:

$$I = A \cdot i_0 \cdot \left[e^{\frac{(1-\alpha)\cdot n\cdot F\cdot (E-E_{eq})}{R\cdot T}} - e^{\frac{-\alpha\cdot n\cdot F\cdot (E-E_{eq})}{R\cdot T}} \right] \quad (1)$$

where I is the electrode current, i_0 the current exchange density, A the electrode surface area, E the electrode potential, E_{eq} the equilibrium potential, T the absolute temperature, n the number of electrons involved, F the Faraday constant, R the universal gas constant and α the charge transfer coefficient [21].

Such equation is always correct for the whole over-potential range applied but, if either cathodic or anodic over-potential is higher than $0.05\ \mathrm{V}$, the first or the second term of the equation can be respectively neglected. This simplification leads to the following linearized equation, known as Tafel equation:

$$\eta = a \pm b \cdot log(i) \quad (2)$$

where η is the over-potential, *a* and *b* are Tafel constant and *i* the current density [21].

At this point it is possible to derive the Corrosion Current (I_{corr}) and Corrosion Potential (E_{corr}) for the different samples from the polarization curves by means of Tafel extrapolation method. IviumSoftware 4.933 was employed to compute the values of the two parameters. Reported data for each sample are the average values computed in the three repetitions.

IV. RESULTS

Potentiodynamic polarization curves are shown in Fig. 3. As can be seen, different behaviours can be found among the samples. Actually, the curves obtained for samples A and C are shifted towards lower current density values, which means that their corrosion kinetic, for both cathodic and anodic reaction, is slower than for the samples B and D. Such trend is also confirmed by the high repeatability of the measurements (all the 3 curves of each samples are almost overlapped) and by the results derived by Tafel extrapolation. As a matter of fact I_{corr} computation shows two different behaviours: both samples A and C achieve low current density values, $0.44\ \mu\mathrm{A/cm^2}$ and $0.39\ \mu\mathrm{A/cm^2}$ respectively, while samples B and D exhibit I_{corr} values more than twice as high as the others, that is $1.12\ \mu\mathrm{A/cm^2}$ and $0.82\ \mu\mathrm{A/cm^2}$ respectively. Due to the proportionality between I_{corr} and the corrosion rate, it is thus possible to associate a faster corrosion kinetics to samples B and D.

Such results can be correlated to the porosity levels computed in Section II, as both sample A and C exhibit the higher density levels. In particular, in this study 3 porosity factors have been taken in consideration:

- Surface percentage occupied by pores: this parameter is important in order to understand the quality of the sample and its final density
- Pore average area: presence of bigger pores strongly affects the mechanical properties but it also exposes more surface area that can be affected by corrosion processes

- Number of pores present on the surface: this factor is really important since every pore can act as an initialization point for pitting. So the higher is this value and higher is the possibility of pit formation [22].

The highest I_{corr} was obtained for sample B, even if the lowest density level was achieved by sample D. This can be justified by the fact that porosity plays an important role for corrosion behaviour, but it is not the only factor which affects it. Actually, it is well-know that from different additive manufacturing process parameters it is possible to achieve unique microstructural features that can lead to different mechanical and corrosion properties. Such aspect goes beyond the aim of this study, so it has not been further investigated.

Then, considering samples A and C, a good correlation between the pores density and the corrosion behaviour can be observed, with sample C having the best corrosion resistance. As far as E_{corr} is concerned, it is clear that such parameter, reported in Fig. 4a, is almost not affected by porosity, since average values remain similar (only few millivolts among the different samples).

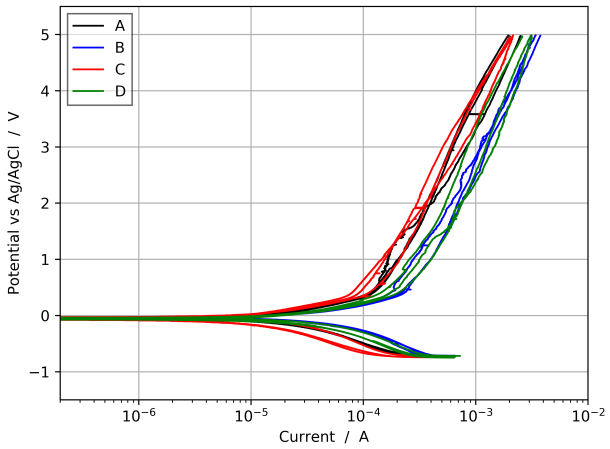

Fig. 3. Polarization curves of the four samples immersed in Hanks' balanced salt solution (three repetitions for each sample). All samples have a surface area equal to 1 cm^2

V. Conclusions

The porosity effect on corrosion resistance of additively manufactured commercially pure titanium was assessed. After characterizing the porosity level in four samples obtained with different process variables, electrochemical behaviour was evaluated using potenziodynamic polarization measurements. Results showed that a higher porosity level leads to a faster kinetics in the corrosion process, which was studied by means of the corrosion current, computed using the Tafel extrapolation method. An important role is also played by number of pores that are present in the sample. Actually, as already reported in literature, they can act as initiation points for pitting, leading to a worse corrosion resistance for the material. These preliminary results can help in the understanding of the corrosion resistance of commercially pure titanium, giving new perspectives for the exploitation in the biomedical field.

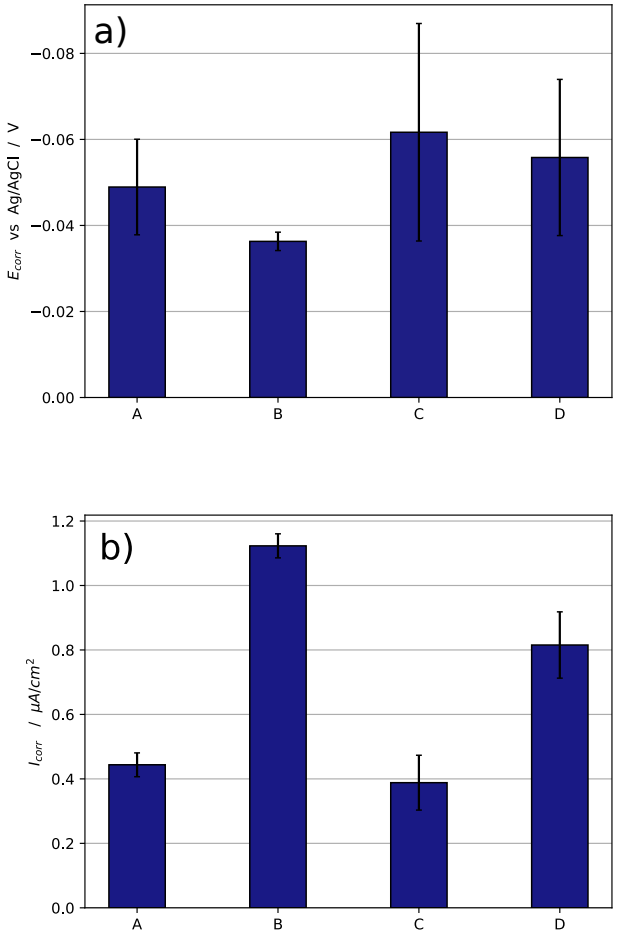

Fig. 4. Parameters derived from Tafel extrapolation method: a) E_{corr} vs Ag/AgCl potential b) I_{corr}. Reported data for each sample are the average values computed in the three repetitions.

References

[1] C. Kuphasuk, Y. Oshida, C. J. Andres, S. T. Hovijitra, M. T. Barco, D. T. Brown, "Electrochemical corrosion of titanium and titanium-based alloys", The Journal of Prosthetic Dentistry, vol 85, no. 2, pp. 195-202, 2001.

[2] W. Geurtsen, "Biocompatibility of dental casting alloys", Critical Reviews in Oral Biology and Medicine, vol 13, pp. 71-84, 2002.

[3] O. E.M. Pohler, "Unalloyed titanium for implants in bone surgery", Injury, vol 31, pp. SD 7-13, 2000.

[4] F. A. Shah, M. Trobos, P. Thomsen, A. Palmquist, "Commercially pure titanium (cp-Ti) versus titanium alloy (Ti6Al4V) materials as bone anchored implants Is one truly better than the other?", Materials Science and Engineering C, vol 62, no. 2, pp. 960-966, 2016.

[5] G. Andria, F. Attivissimo, A. Di Nisio, A. M. L. Lanzolla, P. Larizza, S. Selicato, "Development and performance evaluation of an electromagnetic tracking system for surgery navigation", Measurement, vol 148, pp. 1-7, 2019.

[6] D. Prando, A. Brenna, M. V. Diamanti, S. Beretta, F. Bolzoni, M. Ormellese, M. Pedeferri, "Corrosion of titanium: Part 1: aggressive environments and main forms of degradation", J Appl Biomater Funct Mater, vol 15, no. 4, pp. e291-e302, 2017.

[7] G. Mabilleau, S. Bourdon, M.L. Joly-Guillou, R. Filmon, M.F. Basl, D. Chappard, "Influence of fluoride, hydrogen peroxide and lactic acid on the corrosion resistance of commercially pure titanium", Acta Biomaterialia, vol 2, pp. 121-129, 2006.

[8] G. Sander, J. Tan, P. Balan, Gharbi, D.R. Feenstra, L. Singer, S. Thomas, R.G. Kelly, J.R. Scully, N. Birbilis, "Corrosion of Additively Manufactured Alloys: A Review", Corrosion, vol 74, no. 12, pp. 1318-1350, 2018.

[9] K. Vanmeensel K. Lietaert, B. Vrancken, S. Dadbakhsh, X. Li, J.-P. Kruth, P. Krakhmalev, I. Yadroitsev, J. Van Humbeeck, "Additively manufactured metals for medical applications", Materials, Processes, Quantifications and Applications, pp. 261-309, 2018.

[10] T. WangY, Y.ZhuS, Q.Zhang, H.B.Tang, H.M.Wang, "Grain morphology evolution behavior of titanium alloy components during laser melting deposition additive manufacturing", Journal of Alloys and Compounds, vol 632, pp. 505-513, 2015.

[11] P.A.Kobryna, E.H.Moorea, S.L.Semiatina, "The effect of laser power and traverse speed on microstructure, porosity, and build height in laser-deposited Ti-6Al-4V", Scripta Materialia, vol 43, no. 4, pp. 299-305, 2000.

[12] T.-M. Chiu, M. Mahmoudi, W. Dai, A. Elwany, H. Liang, H. Castaneda, "Corrosion assessment of Ti-6Al-4V fabricated using laser powder-bed fusion additive manufacturing", Electrochimica Acta, vol 279, pp. 143-151, 2018.

[13] N. Dai, L.-C. Zhang, J. Zhang, X. Zhang, Q. Ni, Y. Chen, M. Wu, C. Yang, "Distinction in corrosion resistance of selective laser melted Ti-6Al-4V alloy on different planes", Corrosion Science, vol 111, pp. 703-710, 2016.

[14] E. Pehlivan, M. Daniel, J. Dzugan, "Additively Manufactured CP-Ti (Grade 2) Single Strut Size Effect of Mechanical Response Under Building Direction", IOP Conference Series: Mater. Sci. Eng., vol 461, pp. 960-966, 2018.

[15] N. Dai, L.-C. Zhang, J. Zhang, X. Zhang, Q. Ni, Y. Chen, M. Wu, C. Yang, "Distinction in corrosion resistance of selective laser melted Ti-6Al-4V alloy on different planes", Corrosion Science, vol 111, pp. 703-710, 2016.

[16] N. Vyas, R. L. Sammons, O. Addison, H. Dehghani, A. D. Walmsley, "A quantitative method to measure biofilm removal efficiency from complex biomaterial surfaces using SEM and image analysis", Scientific Reports, volume 6, pp. 1-10, 2016.

[17] I. Arganda-Carreras, A. Cardona, V. Kaynig, J. Schindelin et al., Trainable weka segmentation. http://fiji.sc/Trainable_Weka_Segmentation , Date of access: 02-02-2020 (2019).

[18] L. Iannucci, L. Lombardo, M. Parvis, P. Cristiani, R. Basseguy, E. Angelini, S. Grassini, "An imaging system for microbial corrosion analysis", 2019 IEEE International Instrumentation and Measurement Technology Conference (I2MTC), Auckland, New Zealand, 2019, pp. 1-6

[19] W. Yuan, H. Chen, T. Cheng, Q. Wei, "Effects of laser scanning speeds on different states of the molten pool during selective laser melting: Simulation and experiment", Materials and Design, vol 189, pp. 1-10, 2020.

[20] L. Iannucci, M. Parvis, E. Di Francia, S. Grassini, "iHomeX: An Internet-Enabled Laboratory for Long-Term Experiment Management", IEEE Transactions on Instrumentation and Measurement, vol 67, no. 5, pp. 1142-1149, 2018.

[21] M. G. Fontana, "Corrosion engineering", McGraw-Hill, 3rd edition, Boston (MA), 1986.

[22] C. Ornek, "Additive manufacturing - a general corrosion perspective", Corrosion Engineering, Science and Technology, vol 53, no. 7, pp. 531-535, 2018.